ACCURATE OBSERVER FOR MULTI-FAULT DETECTION AND ISOLATION IN TIME VARYING SYSTEMS USING FAULT CHARACTERIZATION

Ryadh Hadj Mokhneche and Hichem Maaref
Laboratoire Systèmes Complexes
Université d'Evry - CNRS FRE2494
40 rue du Pelvoux 91020 Evry, France

Keywords: Multi-Fault Detection, Multi-Fault Observer, Fault isolation, Fault characterization, Time varying systems.

Abstract: The usual observers up to now allowed the detection of faults in a parameter system via residue signals where each one is judicious to detect one or more faults. However in the event of occurrence of several faults on the same parameter, the residue signal of this observer will be able to detect them only if those are sufficiently spaced in time. But in the event of their occurrence at very close moments, they will be overlapped or compared to only one fault and having a more significant amplitude. Thus, if a possible fault compensation is carried out, it will be incorrect.
In this paper, it is proposed then an accurate observer for fault detection and isolation for one or several faults on a same parameter and with a significant resolution. First, the characteristics of fault are shown to be used in a goal of determinating the types of possible detections. An application of simulation is detailed and achieved for fault detection in a sensor-based system, where the results are discussed. The succession effect of several faults is tested, at one time or different times, on the amplitude, sign and general form of these faults. In the end, the resolution of this observer is highlighted where a comparison between the usual observer and the accurate observer is discussed.

1 INTRODUCTION

The problem of multi-fault detection in time variant systems have always represented a subject of topicality as studied in (V. Venkatasubramanian and Kavuri, 2003a), (V. Venkatasubramanian and Kavuri, 2003b), (V. Venkatasubramanian and Yin, 2003), (P. Zhang and Zhou, 2001), (R. Hadj Mokhneche and Vigneron, 2005), (Kuo and Golnaraghi, 2003) and (Rosenwasser and Lampe, 2000).

Several works was completed during the two last decades for only the fault detection problem in dynamical systems with simple or complex structure (Gertler and Dekker, 2002), (A. Saberi and Niemann, 2000), that improve the importance of this problem witch becomes increasingly current. The borders between the various alternatives of approaches are fuzzy; and some recent work showed that the majority of methods are closely related the ones to the others (Kuo and Golnaraghi, 2003). There are several approaches, methods and strategies for fault detection and isolation, and the most used ones are observer-based approaches (V. Venkatasubramanian and Kavuri, 2003b).

Designing multi-fault detection system and its isolation require a suitable compromise between raising the sensitivity to faults and increasing the robustness to unknown disturbances (Rosenwasser and Lampe, 2000). The most important part of model-based approaches for multi-fault detection is the residual generation problem and among the various existing methods the most used are the observer-based plans (Zhang, 2000) (Frisk and Nyberg, 2001). The signal residue can detect more than one fault successively, but if these faults occur at very close moments the observer compares them to only one fault with characteristics different that when these faults are detected separately. Thus, it is proposed an accurate or precise observer which is able to detect these very close faults without change on their amplitude and with a significant resolution.

So, in what follows, the design of this accurate observer is proceeded. Then, a complete simulation on a system with speed observation is achieved. Several comments and descriptions on this accurate observer will be detailed. In the end, a general conclusion on the results is given.

Hadj Mokhneche R. and Maaref H. (2006).
ACCURATE OBSERVER FOR MULTI-FAULT DETECTION AND ISOLATION IN TIME VARYING SYSTEMS USING FAULT CHARACTERIZATION.
In *Proceedings of the Third International Conference on Informatics in Control, Automation and Robotics*, pages 134-141
DOI: 10.5220/0001217201340141
Copyright © SciTePress

2 THE USUAL OBSERVER

It is described in order to determine the system dynamics integrating the observer. It will be explained then its detection capacities limits.

2.1 Linear Case

Let us consider initially a dynamical system where its state feedback control law is given by (Kuo and Golnaraghi, 2003), (Rosenwasser and Lampe, 2000) :

$$u = -Kx \tag{1}$$

u is the system command, K the gain matrix and x the system state. Consider the system :

$$\begin{array}{l} \dot{x} = Ax + Bu \\ y = Cx \end{array} \tag{2}$$

where $y(t)$ is the output, C the application matrix of state and where (A, C) is an observable pair. The observer takes the form :

$$\begin{array}{l} \dot{\hat{x}} = A\hat{x} + Bu \\ \hat{y} = C\hat{x} \end{array} \tag{3}$$

By comparing the measured output with the output computed from the state estimate, this gives

$$\begin{array}{rcl} \tilde{y} & = & y - \hat{y} \\ & = & (Cx) - (C\hat{x}) \\ & = & C\tilde{x} \end{array} \tag{4}$$

Computing the error dynamics once again, that gives

$$\begin{array}{rcl} \dot{\tilde{x}} & = & x - \dot{\hat{x}} \\ & = & (Ax + Bu) - (A\tilde{x} + Bu + G(y - C\hat{x})) \\ & = & (A - GC)\tilde{x} \end{array} \tag{5}$$

Then, the actual state dynamics become

$$\begin{array}{rcl} \dot{x} & = & Ax - BK\hat{x} \\ & = & Ax - BKx + BKx - BK\hat{x} \\ & = & (A - BK)x + BK(x - \hat{x}) \end{array} \tag{6}$$

As computed above, the state estimator error dynamics are

$$\dot{\tilde{x}} = (A - GC)\tilde{x} \tag{7}$$

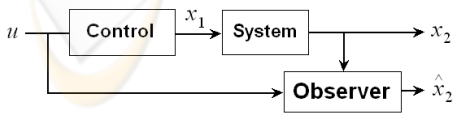

Figure 1: System connected to observer.

With such a dynamics and the observation system showed on the figure (1), the observer generates the signal $r = \hat{y} - y$ (Kuo and Golnaraghi, 2003) which is equal in this case to $\hat{x}_2 - x_2$.

Example of this signal is shown by the figure (2) where all faults have an amplitude value equal to 12. Two faults are simulated at $t = 16s$ but appear as one fault with more significant amplitude, so the two fault amplitudes are in pile up.

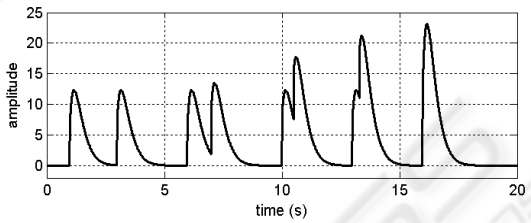

Figure 2: observer signal with multi-faults detection (linear case).

2.2 Non-linear Case

One shall consider non-linear systems ((Jiang and Chowdhury, 2004), (Tan and Edwards, 2003) and (H. Hammouri and Yaagoubi, 1999)) of the form :

$$\left\{ \begin{array}{l} \dot{x}(t) = f(x(t), u(t)); \;\; x(0) = x_0 \\ y(t) = Cx(t) \end{array} \right. \tag{8}$$

Proceeding by analogy to the classical observer design approach in the linear case, one seek an observer of the following form :

$$\left\{ \begin{array}{l} \dot{\hat{x}}(t) = f(\hat{x}(t), u(t)) + g(y(t)) - g(\hat{y}(t)) \\ \hat{y}(t) = C\hat{x}(t) \\ \text{with } \; \hat{x}(0) = \hat{x}_0 \end{array} \right. \tag{9}$$

The state and output errors are defined by :

$$\left\{ \begin{array}{l} e(t) = x(t) - \hat{x}(t) \\ \varepsilon(t) = y(t) - \hat{y}(t) \end{array} \right. \tag{10}$$

By omitting the time variable, the dynamic of estimation error $e(t)$ is then :

$$\dot{e} = f(x, u) - f(\hat{x}, u) - g(y) + g(\hat{y}) \tag{11}$$

Assuming that the observer state converges asymptotically to the state of the system, one can consider the state error (equation 10) in the neighborhood of zero. This allows the use of a first order Taylor expansion of the function f :

$$\begin{array}{rcl} f(x, u) & = & f(\hat{x} + e, u) \\ & = & f(\hat{x}, u) + D_{\hat{x}}(f)\, e \end{array} \tag{12}$$

where $D_{\hat{x}}$; is a differential operator defined by :

$$D_{\hat{x}}(f) = \left. \frac{\partial f(x, u)}{\partial x^T} \right|_{x = \hat{x}} \tag{13}$$

Similarly, for g :

$$g(y) = g(\hat{y}) + D_y(g)\,Ce \tag{14}$$

with :

$$D_y(g) = \left.\frac{\partial g(y)}{\partial y^T}\right|_{y=\hat{y}} \tag{15}$$

Consequently, the dynamic of the estimation error may be rewritten :

$$\dot{e} = [D_{\hat{x}}(f) - D_y(g)\,C]\,e \tag{16}$$

A particular structure of the observer is proposed in order to simplify the calculation of this mapping :

$$\begin{cases} \dot{\hat{x}}(t) = f(\hat{x},u) + R(\hat{x},u)(y-\hat{y}) \\ \hat{y} = C\hat{x} \\ \text{with } \hat{x}(0) = \hat{x}_0 \end{cases} \tag{17}$$

The state error is then solution of the equation :

$$\dot{e} = f(x,u) - f(\hat{x},u) - R(\hat{x},u)(y-\hat{y}) \tag{18}$$

The matricial function $R(\hat{x},u)$ is chosen so that the state error $e(t)$ asymptotically decreases and approaches zero as t tends to infinity. The error $e(t)$ is then considered to be in the neighborhood of zero. By using (12) and (14), a first order Taylor expansion of the function $f(x,u)$ in the neighborhood of the estimated state trajectory $\hat{x}(t)$ is substituted in (18). that gives :

$$\dot{e} = [D_{\hat{x}}(f) - R(\hat{x},u)\,C]\,e \tag{19}$$

The block diagram of the resulting non-linear observer is shown in figure 3 where the time invariant matrix $R(\hat{x},u)$ has to be determined using the algorithm obtained by the derivate of the quadratic Lyapunov function (K. Adjallah and Ragot, 1994).

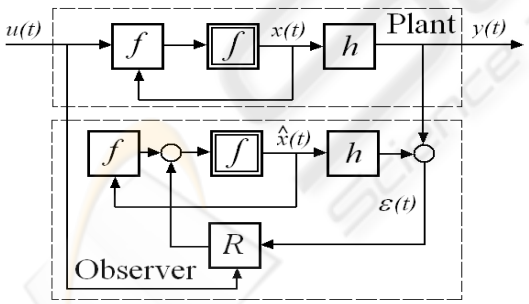

Figure 3: Non-linear observer.

With the observation system showed on figure (3), the observer generates the residual signal shown on figure (4), in absence of noise, where all faults have an amplitude value equal to 7. Two faults are simulated at $t = 5s$ but appear as one fault with more significant amplitude, so the two fault amplitudes are in pile up..

It will be further shown (section 5) that this usual observer provides residue signals limited in precision

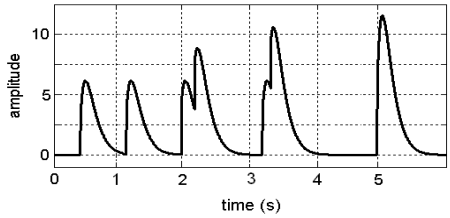

Figure 4: observer signal with multi-faults detection (non linear case).

and that it can not detect two or several very close successive faults (figures 2 and 4) beyond a certain limit which will be defined. Moreover, the amplitudes of the very close faults pile up to form only one fault, which makes incorrect detection. In what follows, a precise observer is carried out and which makes it possible to cure these problems and which has significant characteristics.

3 ACCURATE OBSERVER

When a system parameter undergoes more than one fault at very close moments, the usual observer assimilates all the faults to only one fault with more important amplitude in residue signal. A precise observer must be able to detect them clearly and separately, so to have a high resolution of detection. This leads us to define the types of detection being able to take place during a multi-fault detection.

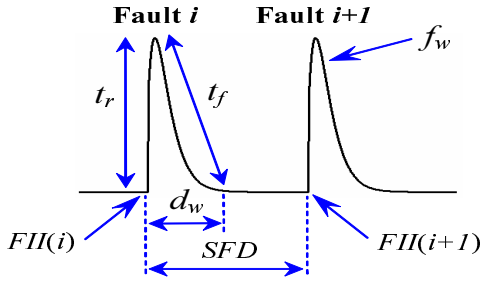

Figure 5: Residue signal with two completely detected faults.

3.1 Types of Detection

Consider the residue signal represented by the figure (5) where the Successive Fault Duration SFD is the duration between two successive completely faults, d_w (wrap duration) $= FID$ (Fault Incidence Duration) is the duration running out between the fault in-

cidence instant FII of fault i and the instant when the residue takes the first value zero or close to zero. t_r and t_f are successively raising time and failing time of the complete fault wrap f_w.

Consider also the figure (6) where MDI is the minimum duration of incidence corresponding to duration between the $FII(i)$ and the finish of the raising time t_r of fault i.

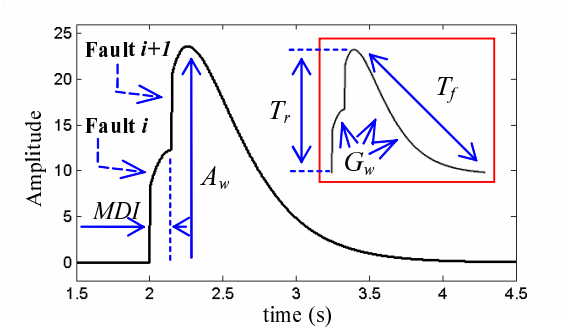

Figure 6: Residue signal with two skewed detected faults.

Three types of two-successive-fault detection can be distinguished :

3.1.1 Complete Fault Detection

In this kind of detection, the two faults are completely detected, i.e. $SFD \geq FID$ (figure 5).

3.1.2 Partial Fault Detection

That means that it satisfied $MDI < SFD < FID$ (figures 5 and 6). The fault $i+1$ occurs during the failing time t_f of fault i, so The fault i is partially detected. The amplitude of fault $i+1$ take a more significant value than envisaged and not representative, what will generate an incorrect eventual compensation for this usual observer.

3.1.3 Skewed Fault Detection

It is obtained where $SFD \leq MDI$ (figure 6). The fault $i+1$ occurs during the raising time t_r of fault i. There is impression thus to detect only one fault and the amplitude corresponds to the pile up of the two faults amplitude. Also, the two faults raising time, successively failing time, pile up to give a total raising time T_r, successively failing time T_f. The two faults wrap are rides and take then a global wrap G_w. This type of detection with usual observer will lead to an incorrect eventual compensation.

3.2 Accurate Observer for Multi-fault Detection

To solve the problems above, it is proposed an accurate observer which uses a modified PID filter and allows the detection of all secondary faults even those occurring during the raising time of the current fault.

The behavior of PID filter can be characterized in terms of its frequency response. A typical curve, as shown in figure (7a), reveals distinct segments named PID elements, each correlating to a different PID term. The damping operation, KD, is a high pass filter with gain that keeps increasing with frequency. This is due to the nature of the derivative function. The effect of increased gain is highly undesirable in systems with noise. In fact, all high frequency noise gets amplified by the KD filter element, further intensifying its damaging effect. This problem can be solved by modifying the PID filter such that the gain curve levels off beyond a given frequency (figure 7b). So, the high frequency gain is limited to a fixed value, thereby reducing the effect of the noise. The gain limit is produced by a low pass filter. The modified compensation technique essentially amounts to a PID filter followed by a low-pass filter.

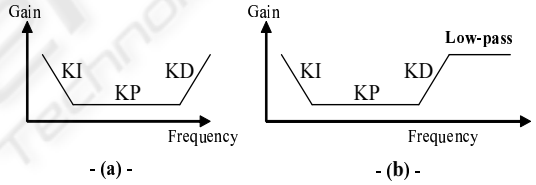

Figure 7: The frequency response of a PID filter (a) and of a low pass filter added to PID filter (b).

With using modified PID filter as explained previously, the noise in the residue will considerably be reduced and the amplitude of residue could be limited. Thus that leads us to obtain a robust observer to noise. The modified PID filter associated to observer give us the accurate observer.

4 APPLICATION

4.1 Presentation

The figure (8) represents a system to observing speed where the system is a sensor-based one. x_1 and x_2 are state variables and x_1 the speed to observe. The observer is designed to follow x_1 by knowing the signals x_2 and u.

Here, the signal x_2 is obtained starting from the signal x_1 using a sensor with transfer function $H(s)$:

$$H(s) = \frac{2-s}{2+s} \tag{20}$$

where s is a symbolic parameter.

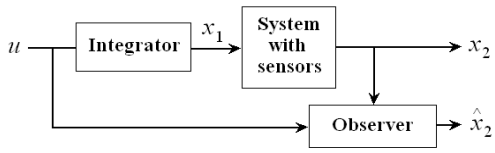

Figure 8: System connected to observer.

The associated equation to integrator block is $\dot{x}_1 = u$. The transfer function of sensor block decay in the following form

$$H(s) = \frac{2-s}{2+s} = \frac{-s-2}{s+2} + \frac{4}{s+2} \tag{21}$$

which a realization of state is

$$\begin{cases} \dot{x}_c = -2x_c + x_1 \\ x_2 = 4x_c - x_1 \end{cases} \tag{22}$$

where x_c is intermediate characteristic variable.

The states of the observer to synthesize are $\hat{x}_1$ and $\hat{x}_2$ which follow the states x_1 and x_2 respectively. After transformations and calculations, an asymptotic observer is looked for by considering the error prediction which is here the considered residue :

$$r = \hat{y} - y = \hat{x}_2 - x_2 \tag{23}$$

5 TESTS AND RESULTS

The diagram of figure (9) shows the simulation scheme of one or several faults (external disturbances) applied to the sensor-based system.

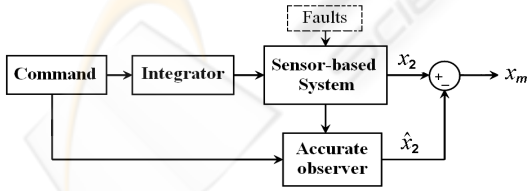

Figure 9: multi-fault system with the observer.

An observer is designed and set to estimate the output signal of the system. It enables us to deduce the predictive error and thus the residue signal x_r of the usual observer and the residue signal x_m of the accurate observer whose PID parameters are judiciously calculated. Simulation is achieved in the single fault case and in the the two or several faults case.

5.1 Single Fault Case

A fault is simulated at $t = 10s$, its effect is visible in sensor signal (fig. 10a) and residue signal (fig. 11).

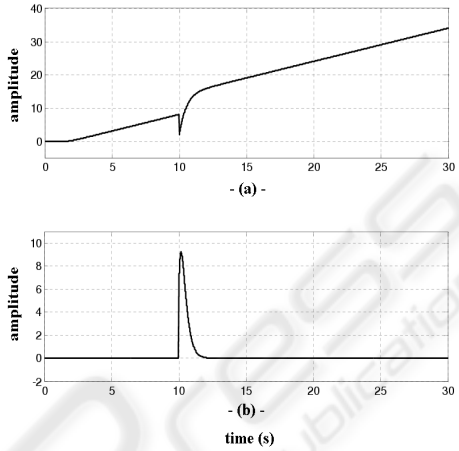

Figure 10: usual observer : Noiseless sensor signal x_2 (a) and noiseless residue signal x_r (b).

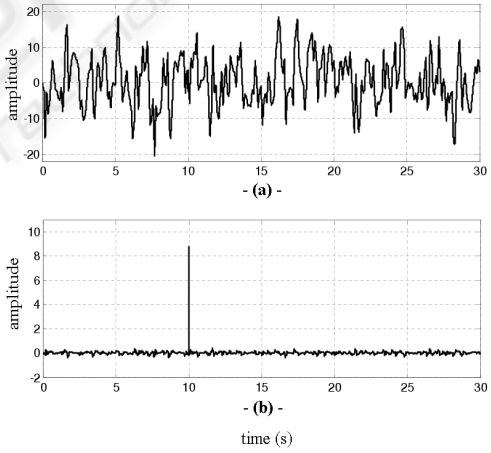

Figure 11: Residue signal in presence of noise : usual observer (a) and accurate observer(b).

In absence of noise : When there are no faults, the residue r tends to zero as ensured by the convergence of the observer. Thus after the transient of the observer, and before the incident of fault, it can be considered that the residue is practically zero. The occurrence of a fault modifies the behavior of the residue signal as shown on figure (10b).

Let us suppose that the fault corresponds to a change in one parameter of the sensor. As the observer generating x_r still relies on the nominal

parameter value, x_r will not remain zero. After a transient of the observer, the residue x_r tends back to zero, as the new value of the estimate parameter is being correctly estimated by the observer. It should be noted that signal x_m is identical to that of x_r except that duration $FID = d_w$ (see figure 5) is very close to zero.

In presence of noise : Now it is assumed that the output measurement x_2 is noise corrupted. If the noise is small compared to the effect of fault on the residue, then the fault detection can still reasonably be performed through visual inspection of the residue. However, if the noise is relatively high, then the change in the behavior of the residue after the occurrence of a fault will be more or less hidden by the noise. The figure (11a) shows the residue signal of noise corrupted usual observer where the fault does not appear.

The figure (11b) shows the signal x_m of noise corrupted accurate observer where the fault is clearly detected with an FID close to zero.

5.2 Two or Several Faults Case

5.2.1 Detection of Distinguished Faults

Initially four faults are simulated, two same faults at the same moment $t = 10s$ and two same others at the same moment $t = 30s$ (figure 12).

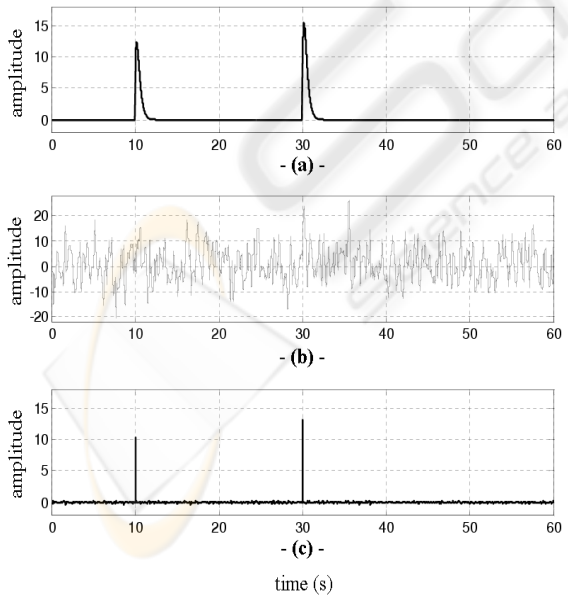

Figure 12: Residue signal in presence of 4 faults (two added by two) : noiseless (a) and noise corrupted (b) usual observer, noise corrupted accurate observer (c).

One remarks that in noiseless usual observer case, the amplitudes of the faults inflicted in the same instant appear in the residue while accumulating in *pile-up* and thus the total amplitude of the residue increased (figure 12a). The figure (12b) shows the noise corrupted usual observer where faults are not detected. In noise corrupted accurate observer case, the faults are clearly detected although there is an increase on amplitude (figure 12c).

While comparing the residue amplitude at instant $t = 10s$ to that at $t = 30s$ of figure (12), the residue amplitude is independent of the occurring moment of fault.

5.2.2 Not Distinguished Faults

For the type of partial detection (figure 13) it was simulated two faults, one at the instant $t = 10s$ with amplitude 12 and the other at the instant $t = 11s$ with amplitude 8.

One can remark that in usual observer case, as far as the second fault is close to the first (figures 13a and 13c), i.e. that FID decreases until reaching the maximum of first fault amplitude, the amplitude of the second fault increases and tends to hide the first one.

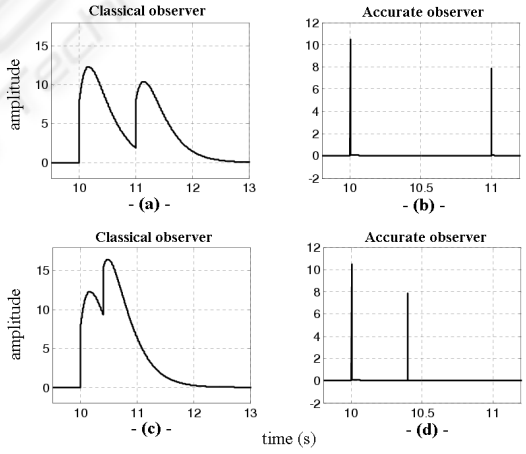

Figure 13: Noiseless residue signals in presence of two faults at very close moments corresponding to partial detection ($MDI < SFD < FID$).

But in the accurate observer case (figures 13b and 13d), the faults are clearly apparent with their exact amplitudes.

Detections seeming like impulses at the instants 10s and 11s (figure 13b) and at the instants 10s and 10.4s (figure 13d), and of all simulations in the accurate observer case, are made up each one of a raising

time and a failing time like those represented on the figures (13g) and (13h).

The simulations of figures (14) and (15) are achieved with tree faults at instant $t = 10s$, $12s$ and $14s$, with amplitudes respectively 7, 15 and 12, in absence of noise. They summarize the three types of detection described in paragraph (3.1), respectively in absence and in presence of noise.

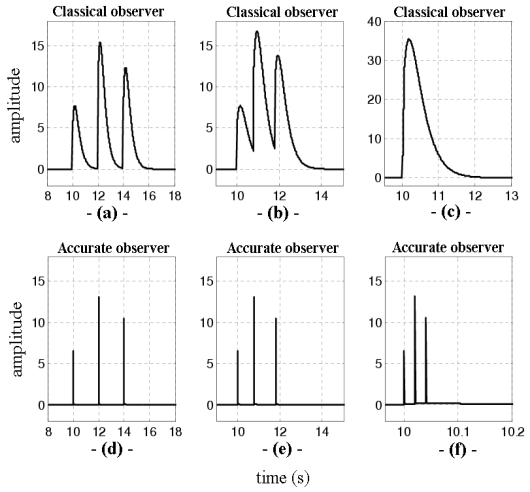

Figure 14: The three types of detection - presence of tree faults at very close moments : Noiseless case.

The figures (14a) and (14b) showed respectively the complete detection with *usual* observer and with accurate observer, where the three faults are clearly detected with exact amplitudes. For the partial fault detection, the simulation is shown on figures (14b) and (14e) where the usual observer detects partially the second and third faults and with an increase in the amplitude, but the accurate observer detects clearly the tree faults and without increase in the amplitude. In case of skewed detection (figures 14c and 14f), the usual observer detects the faults but assimilates them to only one fault instead of three and with a big increase in the amplitude (pile up of the amplitudes of the three faults). The accurate observer detect them all and clearly.

The noise corrupted case for the three types of fault detection is shown on figure (15) and where, in opposite of usual observer, the faults are clearly detected by the accurate observer.

5.3 Observer Resolution

5.3.1 Usual Observer

The limit capacity of usual observer to detect two successive faults in absence of noise is shown on figure

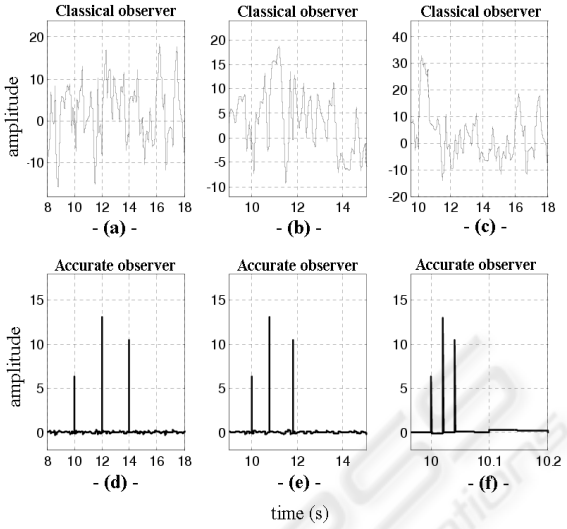

Figure 15: The three types of detection - presence of tree faults at very close moments : Noise corrupted case.

(16a) for the limit skewed detection case ($SFD = MDI$). On figure (16c), for the skewed detection case ($SFD < MDI$), one can remark that there is an impression that it was detected only one fault. In noise corrupted case, there is not faults detected (figures 16b and 16d). One is interested rather in the completely detected faults, thus to FID. This last one is in this usual observer case equal to $2s$ which is enormous. So, if faults occur with $SFD < 2s$ then they will not be correctly detected or not a whole detected.

5.3.2 Accurate Observer

The figures (16g) and (16h) shows the effectiveness of the accurate observer to detect two faults with significant resolution in absence of noise (16g) and in presence of this one (16h). This is valid also for several faults. The resolution of this observer, with step size simulation fixed above, is $FID = 0.002s$ which is twice of step size.

The figures (16e) and (16f) show simulations done respectively in absence and in presence of noise with ($SFD = MDI$) where the MDI reached and corresponding to this limit is $0.2s$. So that, the accurate observer can detect faults occurring with SFD less than the FID of usual observer. The FID founded, corresponding to the limit complete detection of accurate observer is $0.002s$. One can easily remark that this resolution is very precise compared to limit of that from usual observer where the FID is $0.2s$ (figure 14a).

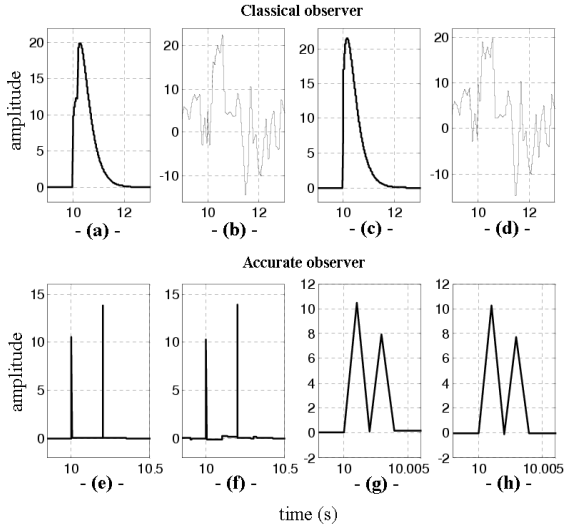

Figure 16: Resolution of the observer in the noiseless and noise corrupted cases.

6 CONCLUSION

It was highlighted, using fault characterization, the detection of several successive faults at same moments and at different moments. It was proved that the moment of fault incidence does not affect the corresponding residue amplitude and it was seen that the observer follows well the sign of the fault. It was proceeded a detection of several successive faults with very close moments, in absence and in presence of noise, corresponding to a resolution with an FID equal to twice of simulation step size. The amplitudes of the faults were respected, thus avoiding the pile up effect due before to the SFD durations which were lower than MDI durations. The signs of the faults amplitudes were also respected, thus allowing a correct eventual future compensation by taking into account the sign of the residue signal.

Three important characteristics of this accurate observer can be noted. The first one is its robustness to noise as shown in different preceding simulations, the second one concern the amplitudes where are conserved and the third one is the resolution where several faults occurring in very close instants are clearly detected. Comparing FID of the usual observer to that of the accurate observer, the second one can detect a significant number of complete faults.

An other interesting characteristic is about the raising and failing times which are very short and right which implies that the accurate observer has significant resolution.

REFERENCES

A. Saberi, A. A. Stoorvogel, P. S. and Niemann, H. (2000). Fundamental problems in fault detection and identification. *International Journal of Robust and Nonlinear Control*, 10:1209–1236.

Frisk, E. and Nyberg, M. (2001). A minimal polynomial basis solution to residual generation for fault diagnosis in linear systems. *Automatica*, 37:1417–1424.

Gertler, J. J. and Dekker, M. (2002). Fault detection and diagnosis in engineering systems. *Control Engineering Practice*, 10:1037–1040.

H. Hammouri, M. K. and Yaagoubi, E. H. E. (1999). Observer-based approach to fault detection and isolation for nonlinear systems. *IEEE Transactions on Automatic Control*, 44:1879–1884.

Jiang, B. and Chowdhury, F. (2004). Observer-based fault diagnosis for a class of nonlinear systems. *Proceeding of the 2004 American Control Conference, Boston, Massachusetts, USA*, 6:5671–5675.

K. Adjallah, D. M. and Ragot, J. (1994). Non-linear observer-based fault detection. *Proceedings of the 3rd IEEE Conference on Control Applications*, 2:1115–1120.

Kuo, B. C. and Golnaraghi, F. (2003). Automatic control systems, 8th edition. *Eds John Wiley and Sons, New York*.

P. Zhang, S. X. Ding, G. Z. W. and Zhou, D. H. (2001). An fdi approach for sampled-data systems. *the 2001 American control conference, Arlington, USA*, pages 2702–2707.

R. Hadj Mokhneche, H. M. and Vigneron, V. (2005). Hybrid algorithms for the parameter estimate using fault detection, and reaching capacities. *The 2nd International Conference on Informatics in Control, Automation and Robotics ICINCO, Barcelona, Spain*, 4:289–293.

Rosenwasser, E. N. and Lampe, B. P. (2000). Computer controlled systems: analysis and design with process-orientated models. *Communications and Control Engineering, Eds. Springer, London, UK*.

Tan, C. P. and Edwards, C. (2003). Sliding mode observers for robust detection and reconstruction of actuator and sensor faults. *International Journal of Robust and Nonlinear Control*, 13:443–463.

V. Venkatasubramanian, R. Rengaswamy, K. Y. and Kavuri, S. N. (2003a). A review of process fault detection and diagnosis. part i: Quantitative model-based methods. *Computers and Chemical Engineering*, 27:293–311.

V. Venkatasubramanian, R. R. and Kavuri, S. N. (2003b). A review of process fault detection and diagnosis. part ii: Qualitative models and search strategies. *Computers and Chemical Engineering*, 27:313–326.

V. Venkatasubramanian, R. Rengaswamy, S. N. K. and Yin, K. (2003). A review of process fault detection and diagnosis. part iii: Process history based methods. *Computers and Chemical Engineering*, 27:327–346.

Zhang, Q. (2000). A new residual generation and evaluation method for detection and isolation of faults in non-linear systems. *International Journal of Adaptive Control and Signal processing*, 14:759–773.